

Supporting Information

Alcohol-Based Adsorption Heat Pumps using Hydrophobic Metal-Organic Frameworks

R.M. Madero-Castro^{a#}, A. Luna-Triguero^{b#}, C. González-Galán^a, J.M. Vicent-Luna^{c*}, S. Calero^{a,c*}

^aDepartment of Physical, Chemical, and Natural Systems, Universidad Pablo de Olavide. Ctra. Utrera km. 1. ES-41013 Seville, Spain.

^bDepartment of Mechanical Engineering, Eindhoven University of Technology, 5600 MB Eindhoven, The Netherlands.

^cMaterials Simulation and Modelling, Department of Applied Physics and Science Education, Eindhoven University of Technology, 5600 MB Eindhoven, The Netherlands.

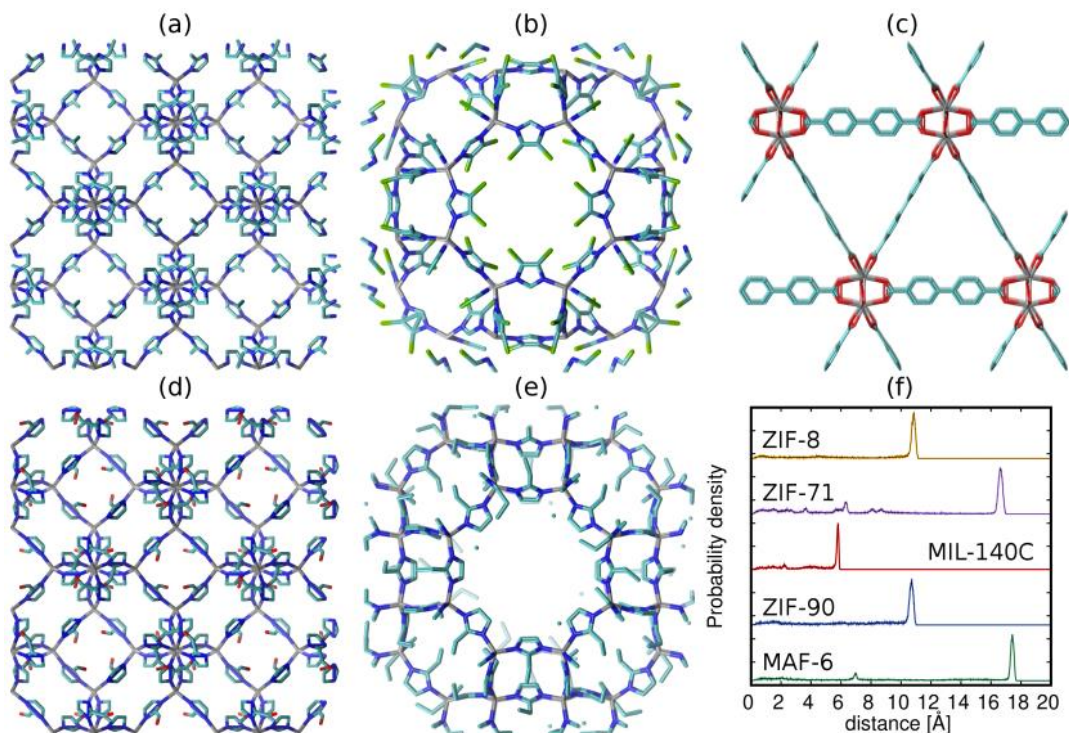


Figure S1. Schematic representation of the framework connectivity of (a) ZIF-8, (b) ZIF-71, (c) MIL-140C, (d) ZIF-90 and (e) MAF-6. (f) Pore Size Distribution. Nitrogen atoms are coloured in blue, carbon atoms in cyan, oxygen atoms in red, chlorine atoms in green, and zirconium and zinc atoms in grey. Hydrogen atoms are omitted for clarity.

Table S1. Structural properties of the selected MOFs, density, pore volume, helium void fraction, surface area, and pore size. Experimental values [1-3] are included between parentheses for comparison.

MOF	Topology	ρ [kg m ⁻³]	V_p [cm ³ g ⁻¹]	HvF	S_A [m ² g ⁻¹]	Pore Size [Å]
ZIF-8	SOD	924.586	0.52 (0.685)[1]	0.484	1732.4 (1696)[1]	10.8
ZIF-90	SOD	988.431	0.51 (0.485)[1]	0.507	1661.3 (1280)[1]	10.7
ZIF-71	RHO	1154.904	0.42 (0.385)[1]	0.496	1379.2 (1183)[1]	16.6
MAF-6	RHO	813.579	0.59 (0.61)[2]	0.482	1664.4 (1695)[2]	17.4
MIL-140C	-	1173.139	0.34 (0.36)[3]	0.400	1298.9 (-)	5.8

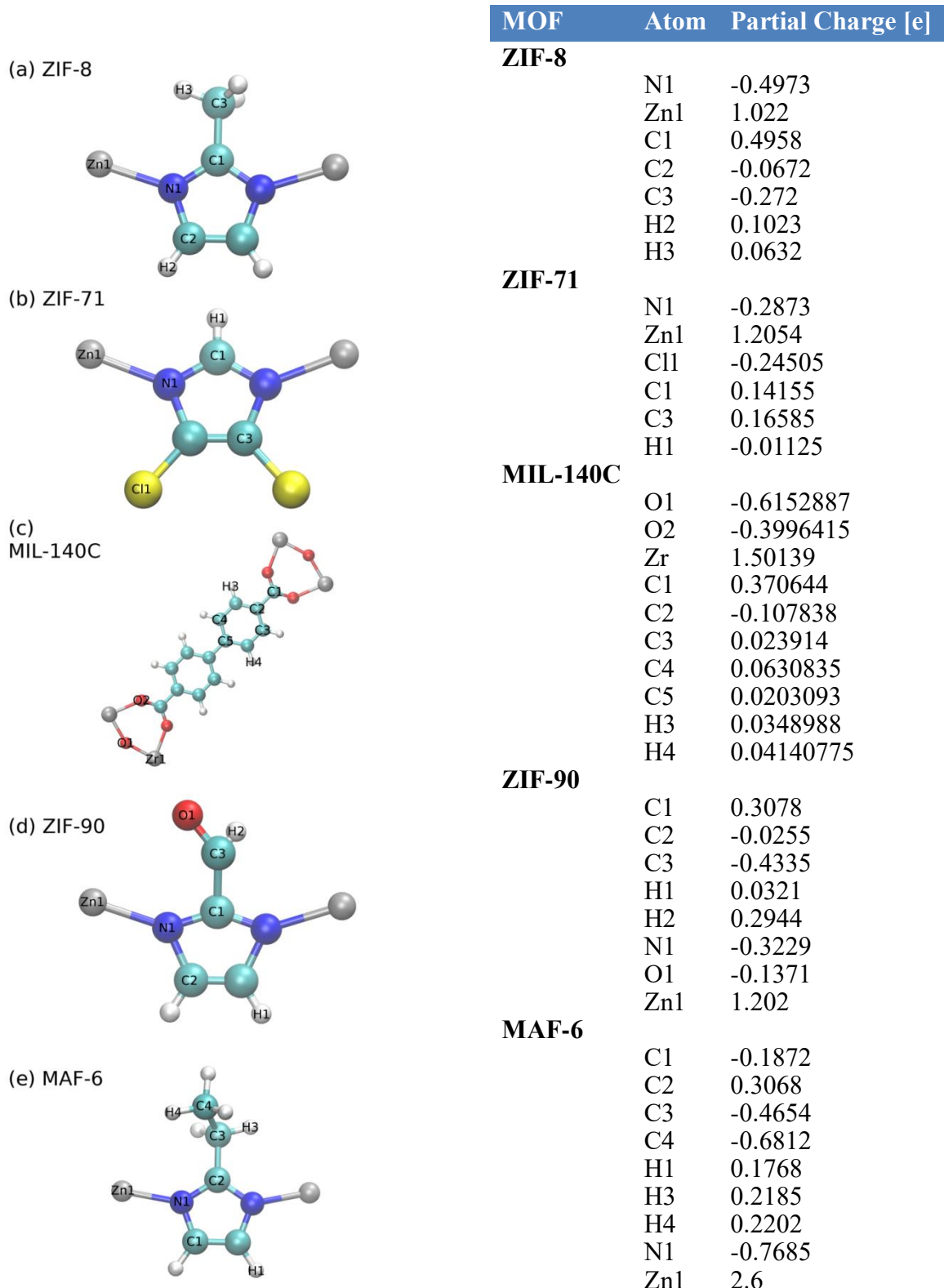


Figure S2. Schematic representation of the organic linkers of (a) of ZIF-8, (b) ZIF-71, (c) MIL-140C, (d) ZIF-90 and (e) MAF-6. Nitrogen atoms in blue, carbon atoms in cyan, oxygen atoms in red, chlorine in yellow, hydrogen in white and zirconium and zinc atoms in grey. Partial charges of atoms of each MOF. MAF-6 charges have been taken from the literature.[4]

Table S2. Equilibrium adsorption conditions of methanol and ethanol for the selected MOFs.

MOF	Isotherm, Temperature [K]		Isobar, Pressure [kPa]	
	Methanol	Ethanol	Methanol	Ethanol
ZIF-8	298	298	5	0.8
	308	308		
ZIF-71	298	298	8	4
	308	308		
MIL-140C	298	298	1.5	4
ZIF-90	298	298	10	3
	308	308		
MAF-6	298	298	10	2.5

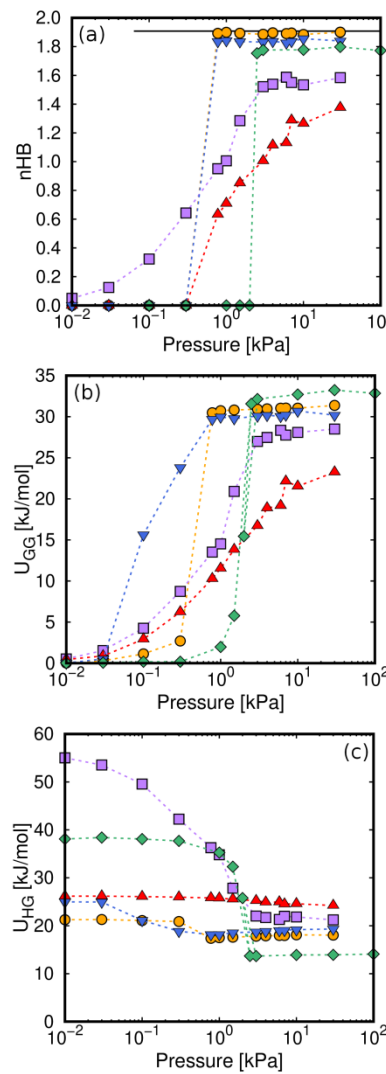


Figure S3 (a) nHB, (b) guest-guest interactions, and (c) host-guest interactions for ethanol as a function of the pressure. Non-depicted error bars denotes fluctuations smaller than symbol size.

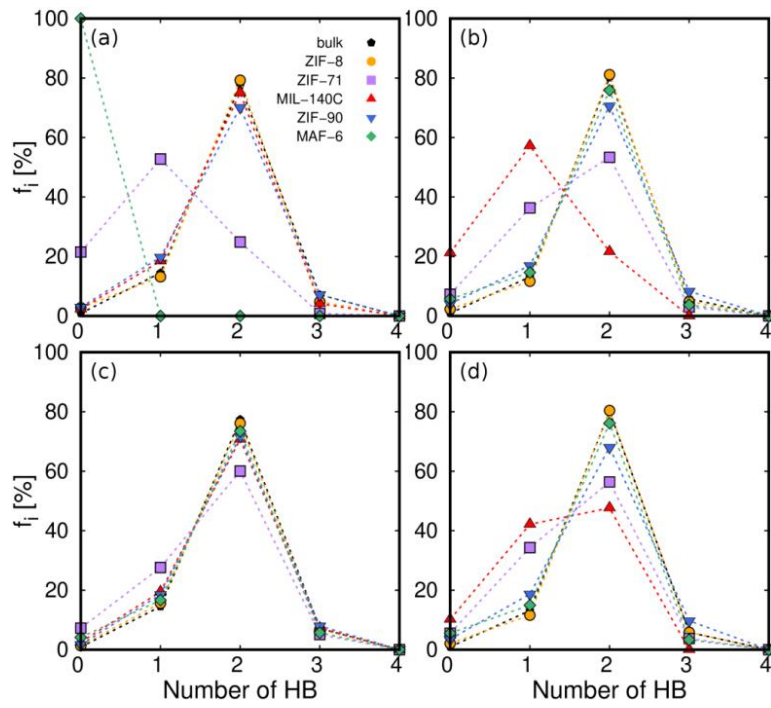


Figure S4 f_i (percentage of molecules with n HBs) of (a) methanol and (b) ethanol at 3kPa. (c, d) the same at saturation conditions. Non-depicted error bars denotes fluctuations smaller than symbol size.

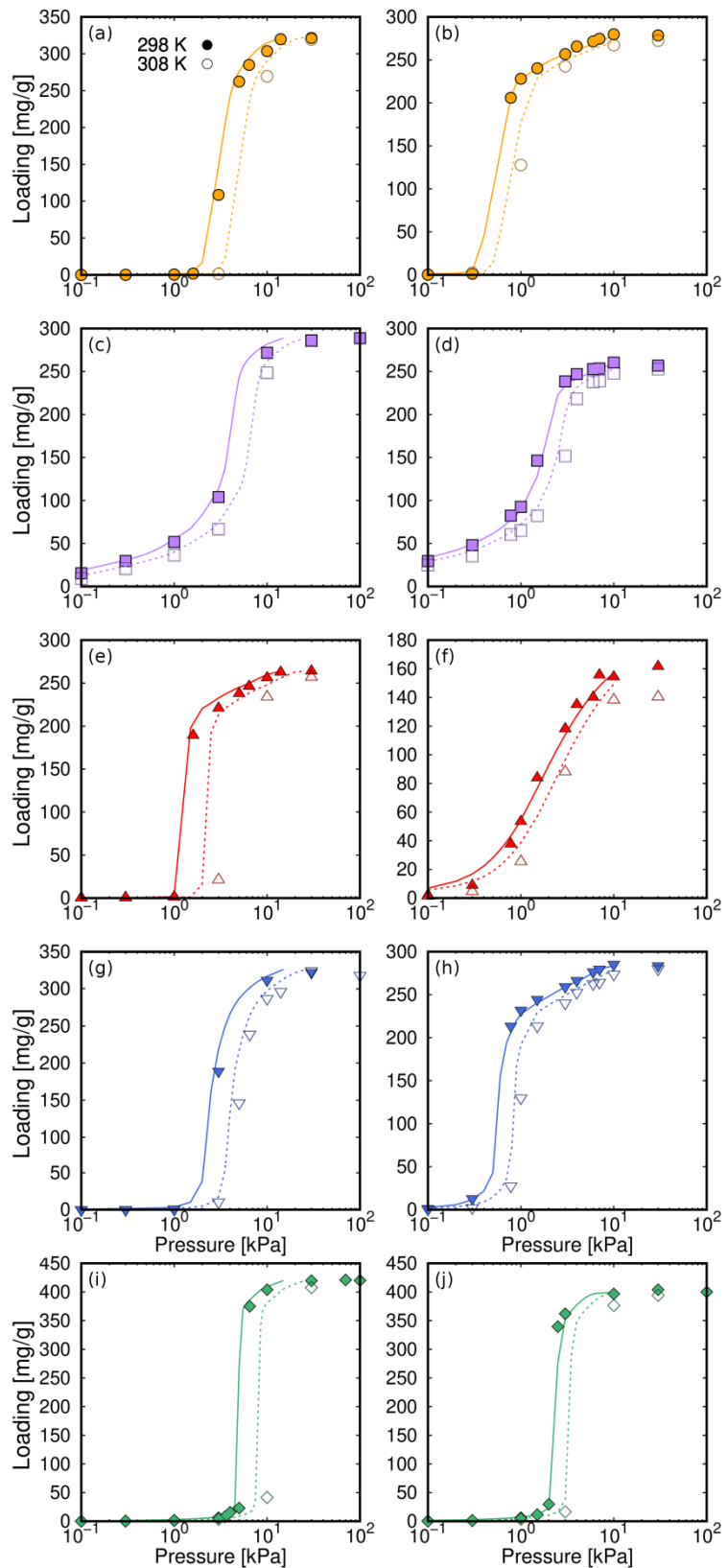


Figure S5 Adsorption isotherms calculated with GCMC simulations (symbols) and from the characteristic curve (lines) of methanol (left column) and ethanol (right column) in (a, b) ZIF-8, (c, d) ZIF-71, (e, f) MIL-140C, (g, h) ZIF-90, and (i, j) MAF-6 at 298 K and 308 K.

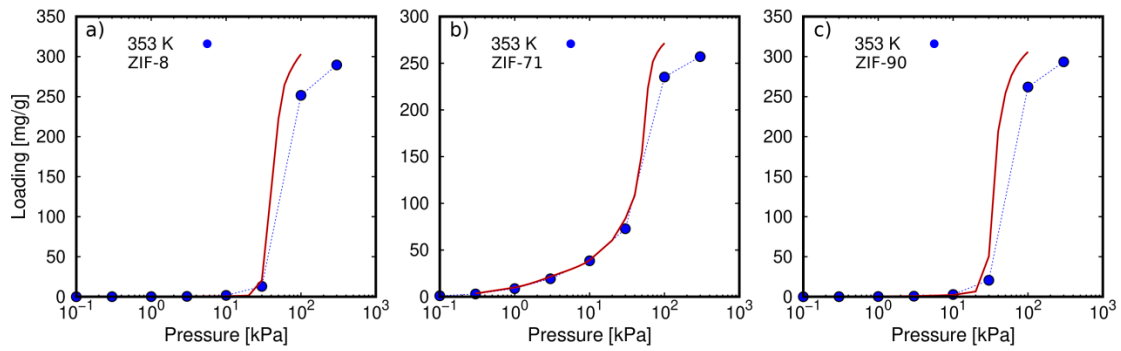


Figure S6. Adsorption isotherms calculated with GCMC simulations (symbols) and from the characteristic curve (lines) of methanol at 353 K in (a) ZIF-8, (b) ZIF-71, and (c) ZIF-90.

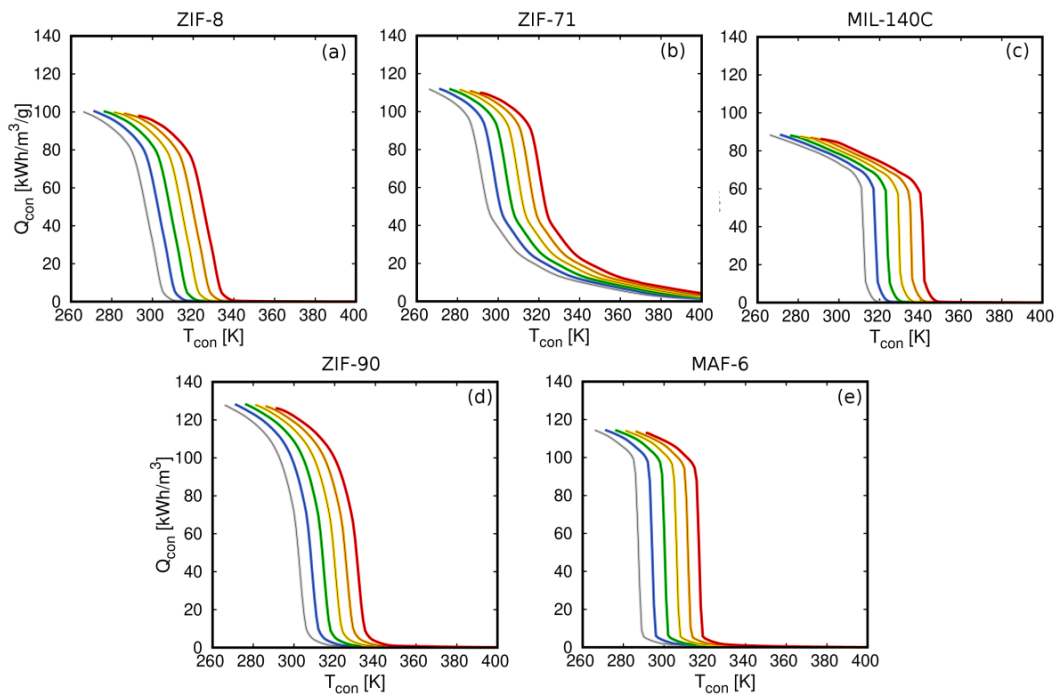


Figure S7. Volumetric heat energy transferred to the condenser (Q_{con}) per unit of volume of MOF using methanol in all MOFs with variation of the temperature of the evaporator assuming full desorption.

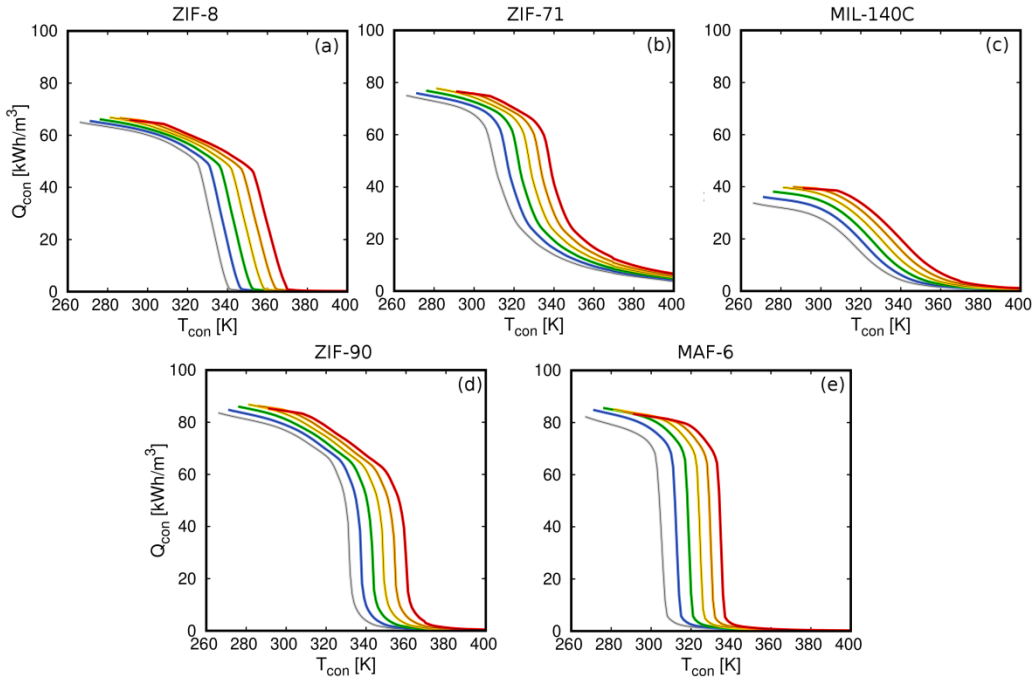


Figure S8. Volumetric heat energy transferred to the condenser (Q_{con}) per unit of volume of MOF using ethanol in all MOFs with variation of the temperature of the evaporator assuming full desorption.

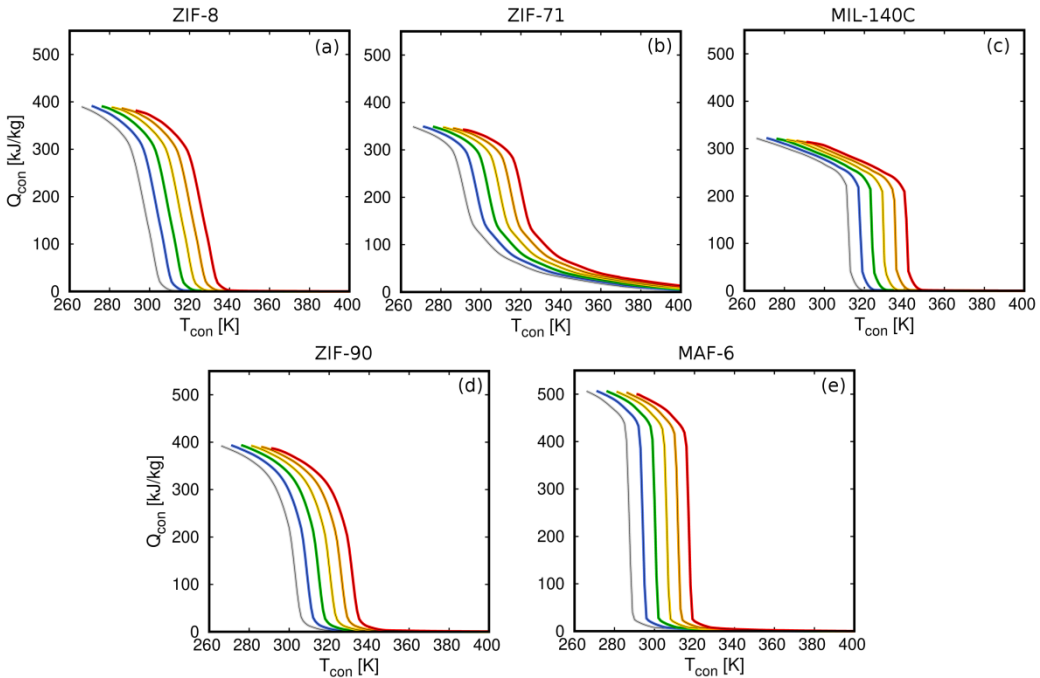


Figure S9. Gravimetric heat energy transferred to the condenser (Q_{con}) per unit of volume of MOF using methanol in all MOFs with variation of the temperature of the evaporator assuming full desorption.

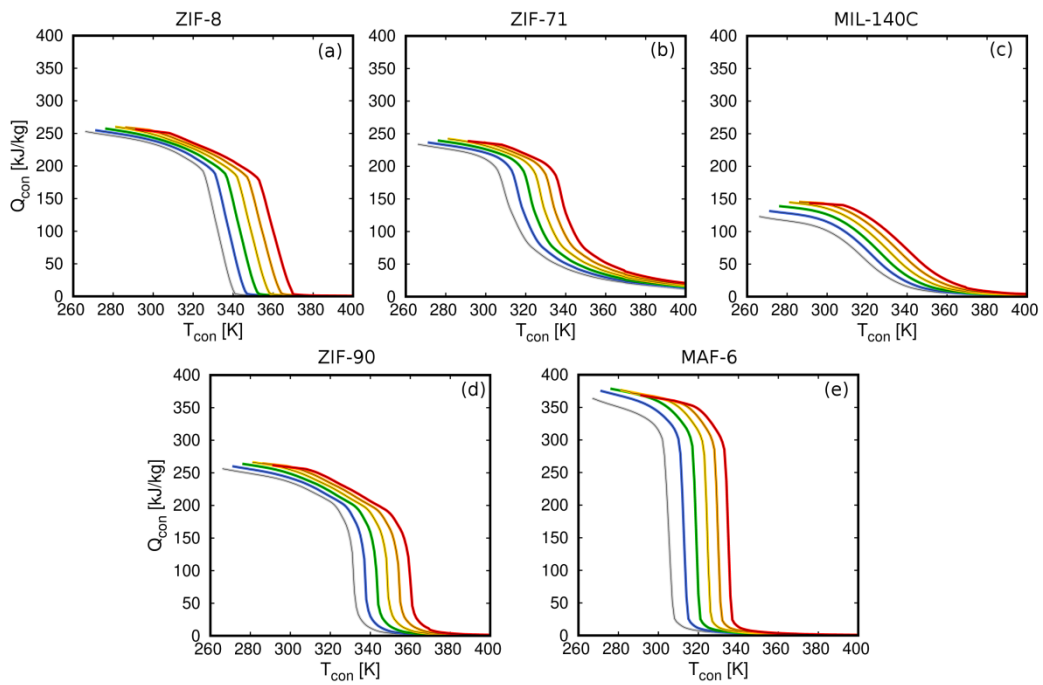


Figure S10. Gravimetric heat energy transferred to the condenser (Q_{con}) per unit of volume of MOF using ethanol in all MOFs with variation of the temperature of the evaporator assuming full desorption.

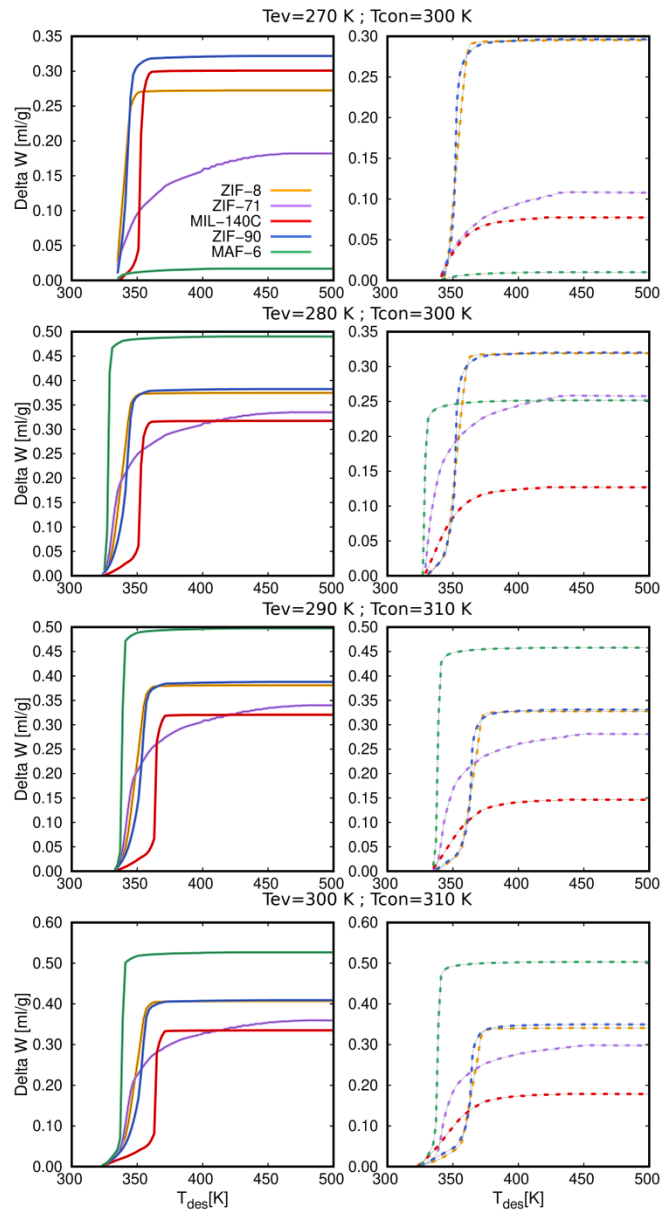


Figure S11. Deliverable capacity for methanol (solid lines) and ethanol (dashed lines) as a function of the desorption temperature for varying the temperatures of the evaporator and condenser.

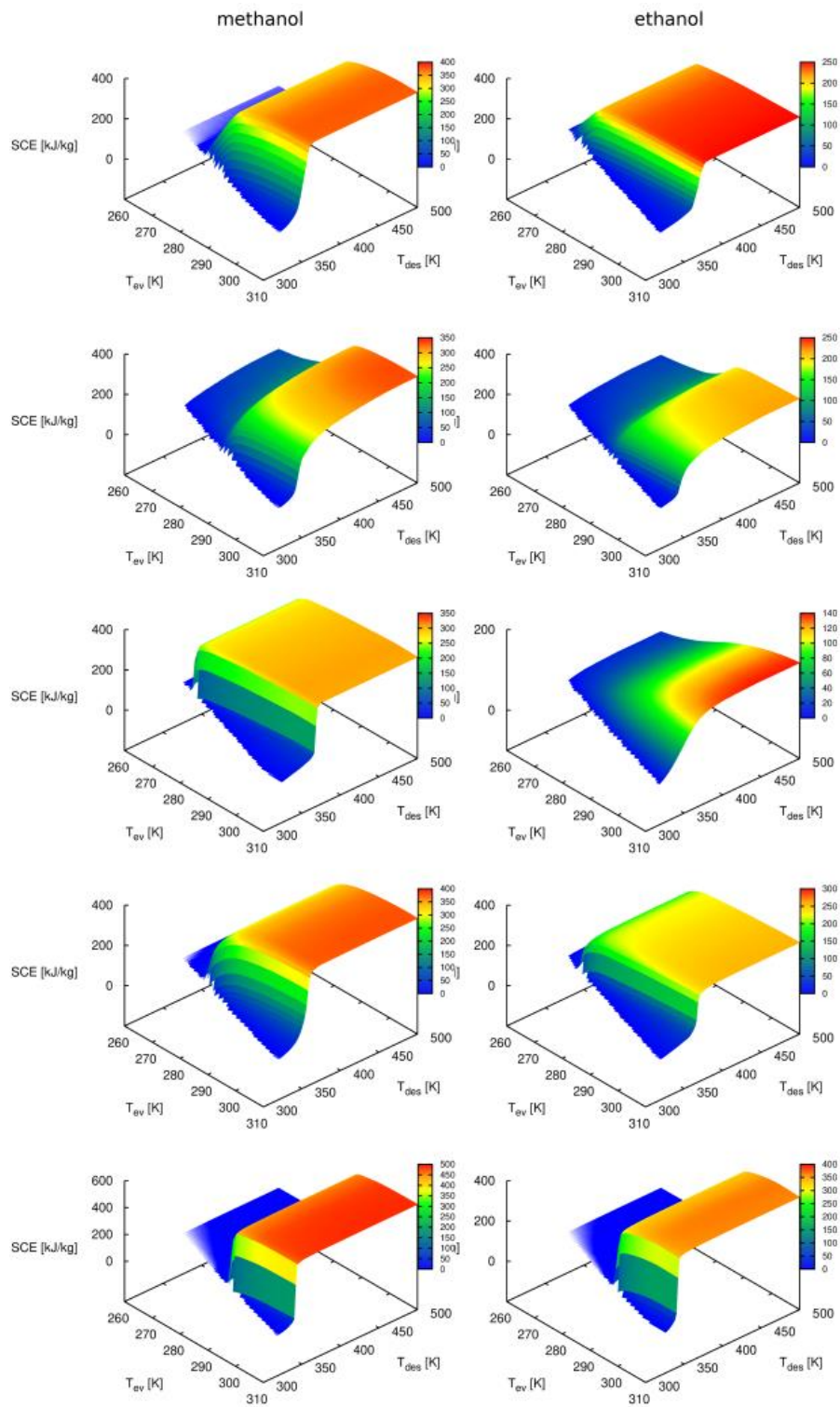


Figure S12. SCE of methanol and ethanol in all MOFs at $T_{\text{con}}=313$ K. From top to bottom, ZIF-8, ZIF-71, MIL-140C, ZIF-90, and MAF-6, respectively.

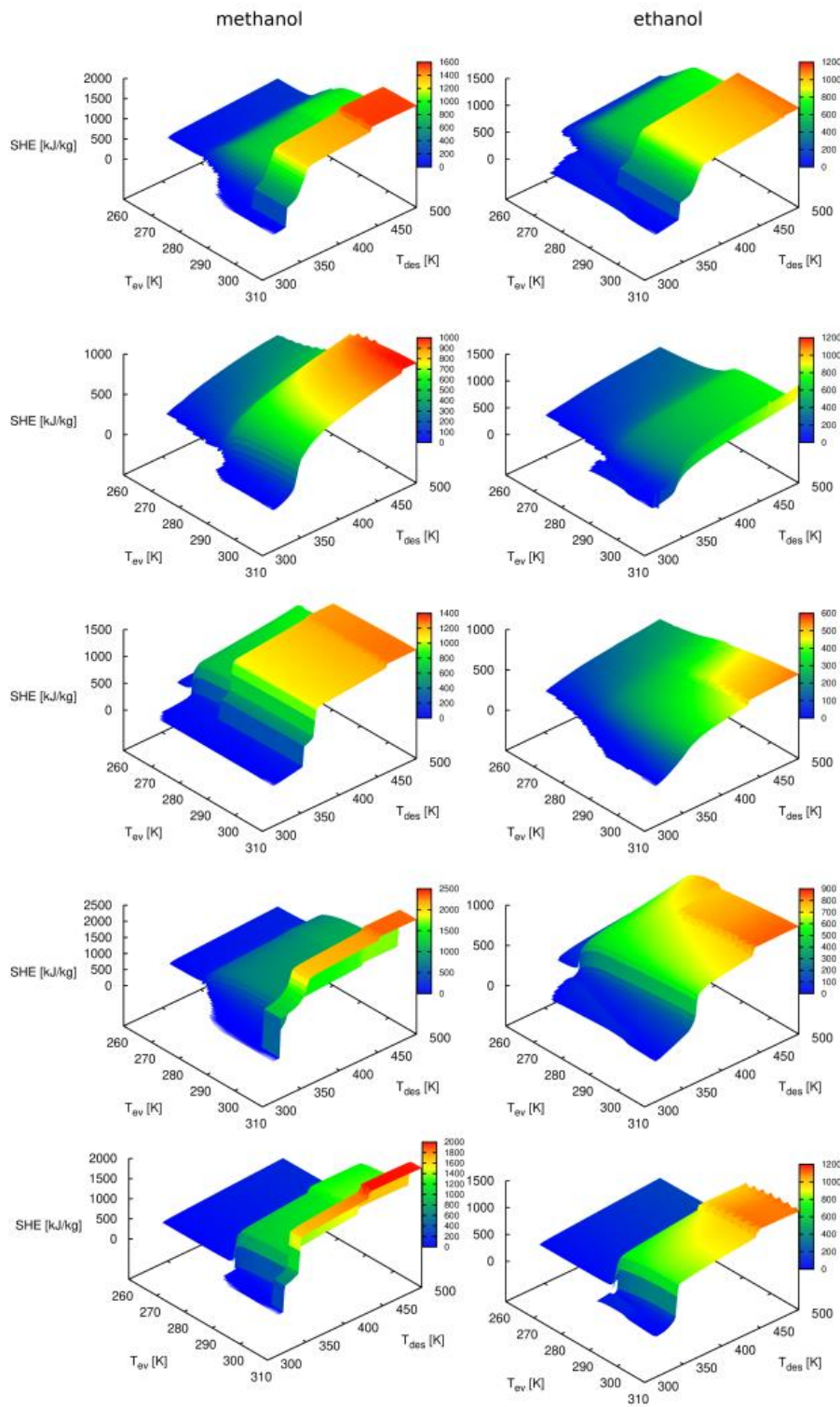


Figure S13. SHE of methanol and ethanol in all MOFs at $T_{\text{con}}=313$ K. From top to bottom, ZIF-8, ZIF-71, MIL-140C, ZIF-90, and MAF-6, respectively.

REFERENCES

- [1] Ke Zhang, Ryan P. Lively, Michelle E. Dose, Andrew J. Brown, Chen Zhang, Jaeyub Chung, Sankar Nair, William J. Koros, and Ronald R. Chance, “Alcohol and water adsorption in zeolitic imidazolate frameworks,” *Chem. Commun.* **49**, 3245–3247 (2013).

- [2] He, C.-T.; Jiang, L.; Ye, Z.-M.; Krishna, R.; Zhong, Z.-S.; Liao, P.-Q.; Xu, J.; Ouyang, G.; Zhang, J.-P.; Chen, X.-M. Exceptional Hydrophobicity of a Large-Pore Metal-Organic Zeolite. *J. Am. Chem. Soc.* **137**, 7217–7223 (2015).
- [3] Martijn F. de Lange, Benjamin L. van Velzen, Coen P. Ottevanger, Karlijn J. F. M. Verouden, Li-Chiang Lin, Thijs J. H. Vlugt, Jorge Gascon, and Freek Kapteijn, “Metal–organic frameworks in adsorption-driven heat pumps: The potential of alcohols as working fluids,” *Langmuir* **31**, 12783–12796 (2015).
- [4] Juan Jose Gutierrez-Sevillano, Sofia Calero, Conchi O. Ania, Jose B. Parra, Freek Kapteijn, Jorge Gascon, and Said Hamad, “Toward a transferable set of charges to model zeolitic imidazolate frameworks: Combined experimental–theoretical research,” *J. Phys. Chem. C* **117**, 466–471 (2013).